WOOD RESEARCH doi.org/10.37763/wr.1336-4561/67.6.10051016
e-ISSN 2729-8906
67(6): 2022 1005-1016 pp.

EXPERIMENTAL VERIFICATION OF THE MODERN SEMI-RIGID TIMBER CONNECTIONS

MATÚŠ NEUSCH, JAROSLAV SANDANUS, KLARA FREUDENBERGER
SLOVAK UNIVERSITY OF TECHNOLOGY IN BRATISLAVA
SLOVAK REPUBLIC

(RECEIVED JUNE 2022)

ABSTRACT

The paper deals with theoretical and experimental research of the timber connections using modern timber connectors Rothoblaas Alumidi. These connectors allow for semi-rigid behaviour of the connections. The paper describes the theoretical background of semi-rigid connections, explains the methods used in the numerical analysis and the design of test connections. The thesis continues with the experimental verification of the designed specimens. The experimental results are compared with the numerical analysis. The findings obtained from the experiment and recommendations for practice are summarized in the conclusion.

KEYWORDS: Dowel-type fasteners, semi-rigid connections, rotational stiffness, slip modulus, experiment.

INTRODUCTION

In engineering practice, the sound design of the load-bearing structure is as important as the sound design of the structural connections. In timber structures, it is often the case that the capacity of the structure limits the capacity of the connections. The design of connections often takes into account hinged action, which means that free rotation is allowed in the connection (Ogrizovic et al. 2017, Zölliget al. 2016). However, modern fasteners allow a certain degree of yielding. Their rotational stiffness is somewhere between hinge action and rigid action (Larsen and Jensen 2000, Dias et al. 2018, Jockwer & Serrano, 2021). We can therefore speak of semi-rigid connections (Sandhaas et al. 2018, Tlustochowicz et al. 2011). Within the experiment, the connection with Alumidi connectors, which are often used to connect beams to the primary structure, was verified. These are aluminium brackets that are placed inside the element to be connected, which implies several advantages. In the experiment, a timber bracket was connected to a glulam beam using this bracket. The deflections of the timber bracket

and the Alumidi bracket itself were read during the experiment. The rotational stiffness of the Alumidi attachment was back calculated based on the deformations of the specimen. Four alternatives of the connection were experimentally verified, which were distinguished by different numbers of fasteners. Each connection was realized on 4 specimens. The experimental results were then confronted with the results of the numerical analysis. The experiment results are described in detail in the conclusion. The research on semi-rigid connections is a continuation of the master thesis (Rácz 2017).

MATERIAL AND METHODS

A bracket to beam connection using Alumidi fastener was chosen as the structural connection. Alumidi is a metal bracket made by pressing from alloy EN AW-6060, with the metallurgical designation $AlMgSi_{0,5}$. The alloy has very good corrosion resistance. Alumidi were available with different heights, namely Alumidi 120 and Alumidi 160 without holes for smooth dowels. At the beginning it is important to divide the connection into two parts, namely the connection of the timber bracket contains of solid structural timber (KVH) to the Alumidi connector - part A, and the connection of the Alumidi to the primary support beam - part B. Two different stiffness values are calculated for the two parts of the connection. In both cases the same calculation procedure applies. The timber bracket length of 0.75 m is connected to the Alumidi using self-drilling dowels SBD Ø 7.5 mm (d_1) with a length of L = 75 mm (Fig. 1). The Alumidi connector is attached to the beam made of glulam GL24h of dimension 140/320 (Fig. 3) using annular ring shank nails with a diameter of d = 4 mm and lengths of L = 60 and 100 mm (Fig. 2). The matter of dowel type connectors has been addressed by several authors (Gečys and Daniūnas 2017, Duchoň 2016, Duchoň et al. 2016, Xu et al. 2012, Guan and Rodd 2001, Serrano et al. 2008, Solarino at el. 2017, Schweigler et al. 2018, Jockwer et al. 2022). The design details follow the design rules and the minimum distances between the fasteners according to Eurocode 5 (EN 1995-1-1 2008). The Alumidi connector is designed in 4 alternatives (variants 1-4), each alternative being tested on 4 specimens. In each alternative, the number of fasteners is increased, which has an effect on the resulting stiffness.

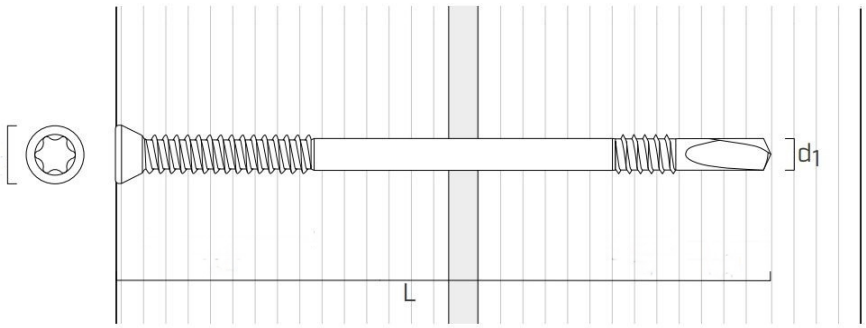

Fig. 1: Self-drilling dowel SBD (Rotho Blaas GmbH, 2019: Plates and connectors for timber).

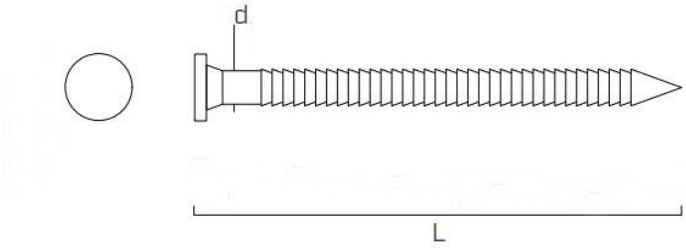

Fig. 2: Annular ring shank nail LBA (Rotho Blaas GmbH, 2019: Screws and connectors for timber).

Due to design possibilities, it was not possible to load the specimens from above, i.e. in the direction of gravity. For this reason, the whole connection was made horizontally mirrored, and the timber bracket was loaded from the bottom side (Fig. 3). The dead load of the timber bracket was negligible in this case. The timber bracket was loaded at a distance of 0.725 m (Fig. 3a) from the edge of the glulam beam from the underside with an ENERPAC RC756 hydraulic press. The press was pressurized by an ENERPAC P-80 hydraulic hand pump.

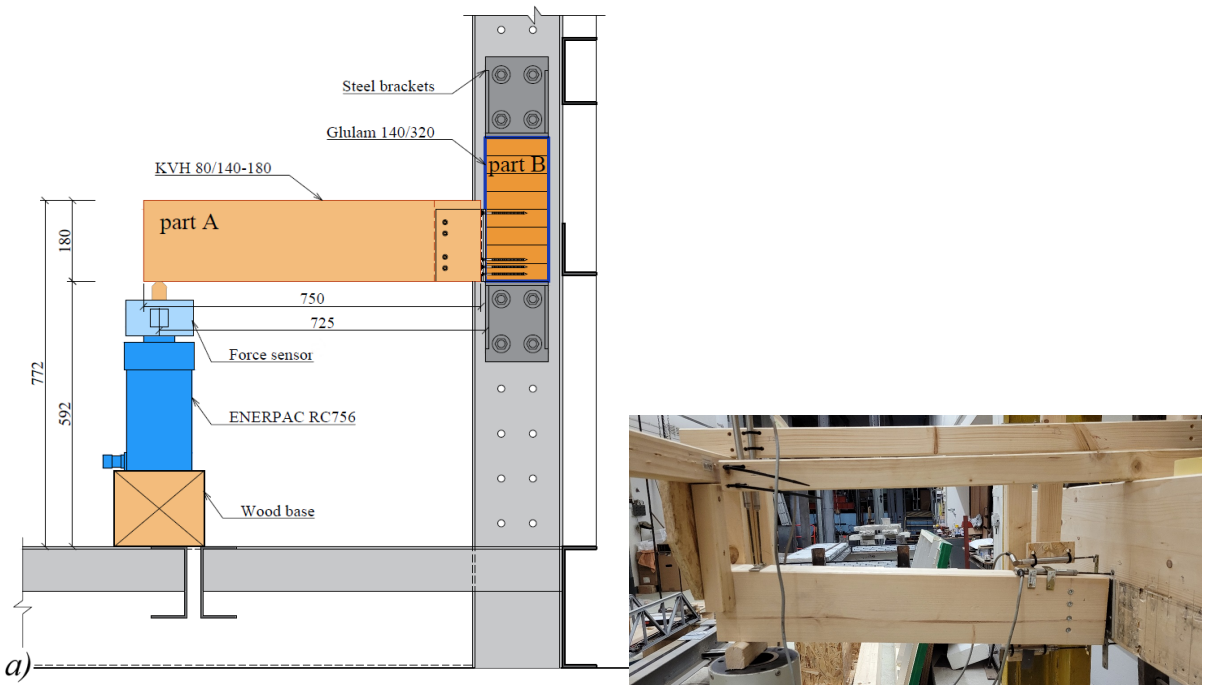

Fig. 3: a) Specimen loading assembly (dimensions in mm). b) The experiment set-up.

The following figures show the designed connections (Fig. 4, Fig. 5) according Eurocodes (EN 1995-1-1 2008, EN 1993-1-1 2005).

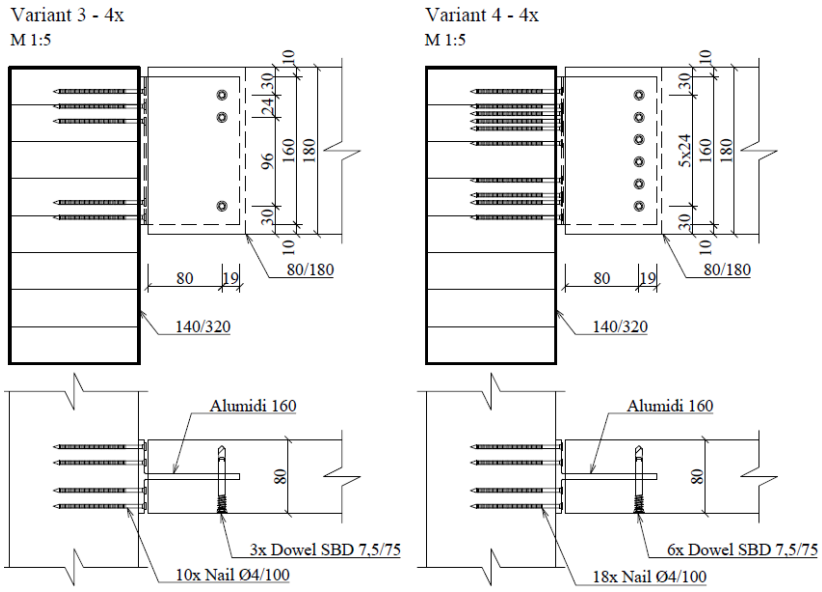

Fig. 4: Designed connections with Alumidi 120 (dimensions in mm).

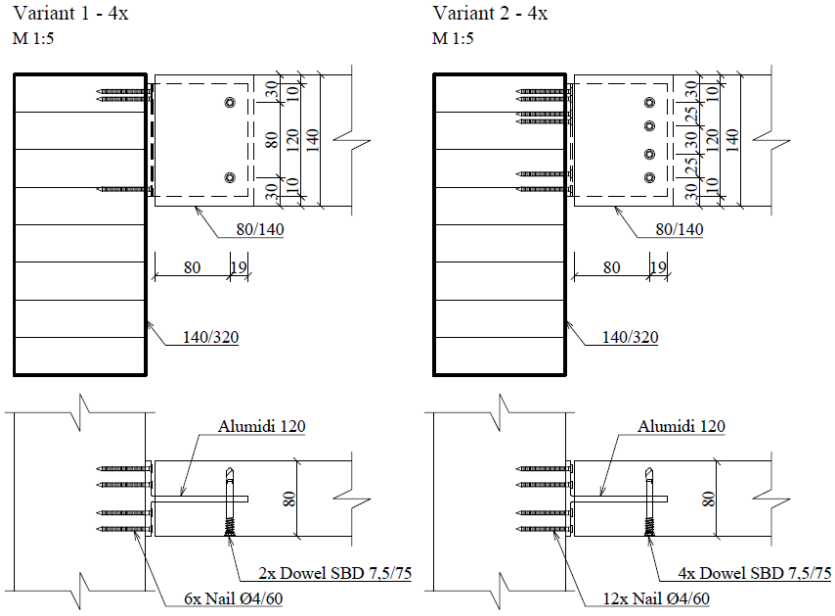

Fig. 5: Designed connections with Alumidi 160 (dimensions in mm).

The deformations of the timber bracket and the deformations of the Alumidi fastener were measured on the specimen. For this purpose, HBM WA-T displacement sensors with a measurable displacement of 5 and 15 cm were used (Fig. 6). Measurements were carried out at the following locations: I1, I2 – vertical deformation at the end of the timber bracket; I3, I4 – horizontal deformation of the timber bracket at the dowel connection from the top side; I5 – horizontal deformation of the timber bracket at the dowel connection from the bottom side, and I6 – horizontal deformation of the Alumidi bracket.

The procedure for the loading the specimen is given by eurocodes (EN 383 2007, EN 380 1998). The loading is carried out in several steps: *(1)* loading of the specimen to a level of $0{,}4*F_{max,est}$ for a duration of 120 s, *(2)* the specimen is then held at $0{,}4*F_{max,est}$ for the duration of

30 s and unloaded to 0,1*$F_{max,est}$ for the duration of 120 sec, *(3)* the specimen is then held at 0,1*$F_{max,est}$ for the duration of 30 s, *(4)* this is followed by loading the specimen to the $F_{max,est}$ for the duration of 300 ± 120 s.

The maximum force with which the specimens could be loaded was defined from the characteristic capacity of the dowel and nail connections.

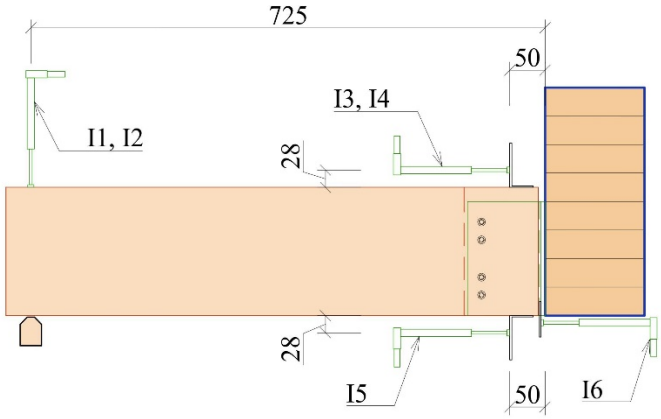

Fig. 6: Location of the displacement sensors (dimensions in mm).

Based on the geometry of the designed connections, the rotational stiffness values of the individual connections were calculated according to the method mentioned in (Schickhofer 2006). The rotational stiffness calculation involves the K_{ser} slip modulus of the connection. For dowel fasteners, the formulas for the calculation of K_{ser} can be found in Eurocode 5, chapter 7.1. The formulas for the calculation of the slip modulus of the annular ring shank nails cannot be found in Eurocode 5. Research on annular ring shank nails has been carries out by several authors (Izzi et al. 2016, 2018). The result is a formula for the calculation of the slip modulus:

$$K_{ser} = \mathrm{k}_h * \mathrm{d} * l \tag{1}$$

where: k_h – modulus of subgrade reaction of timber, k_h = 15 MPa·mm^{-1}, d – diameter of nail (mm), l – effective length (mm).

In the following tables (Tabs. 1-4), the values of the slip modulus and rotational stiffness for the serviceability and ultimate limit state are calculated. The stiffness values are calculated separately for the dowel part of the connection - part A and the nail part of the connection - part B.

Tab. 1: Calculation of the rotational stiffness of the connection with Alumidi 120 for part A.

Variant	Number of dowels	I_p (mm^2)	K_{ser} (N·mm^{-1})	$C_{\psi,MSP}$ (MNm·rad^{-1})	$C_{\psi,MSÚ}$ (MNm·rad^{-1})
V1	2	3200	4303.7	0.0275	0.0184
V2	4	3650	4303.7	0.0314	0.0209

Tab. 2: Calculation of the rotational stiffness of the connection with Alumidi 120 for part B.

Variant	Number of nails	I_p (mm^2)	K_{ser} ($N \cdot mm^{-1}$)	$C_{\psi,MSP}$ ($MNm \cdot rad^{-1}$)	$C_{\psi,MSÚ}$ ($MNm \cdot rad^{-1}$)
V1	6	46848	2884.5	0.1351	0.0901
V2	12	76288	2884.5	0.2201	0.1467

Tab. 3: Calculation of the rotational stiffness of the connection with Alumidi 160 for part A.

Variant	Number of dowels	I_p (mm^2)	K_{ser} ($N \cdot mm^{-1}$)	$C_{\psi,MSP}$ ($MNm \cdot rad^{-1}$)	$C_{\psi,MSÚ}$ ($MNm \cdot rad^{-1}$)
V3	3	8064	4303.7	0.0694	0.0463
V4	6	10080	4303.7	0.0868	0.0578

Tab. 4: Calculation of the rotational stiffness of the connection with Alumidi 160 for part B.

Variant	Number of nails	I_p (mm^2)	K_{ser} ($N \cdot mm^{-1}$)	$C_{\psi,MSP}$ ($MNm \cdot rad^{-1}$)	$C_{\psi,MSÚ}$ ($MNm \cdot rad^{-1}$)
V3	10	100 608	4615.2	0.4643	0.3096
V4	18	168 576	4615.2	0.7780	0.5187

RESULTS AND DISCUSSION

Already with the first specimens, increased deformations of the timber bracket were detected in the experiment. The deformation results at the end of the cantilever were incomparably larger than the deformations from the 3D models with the included connection stiffnesses. According to the observation in the experiment, these deformations were caused by the dowel part of the connection.

During loading, the timber bracket in the dowel connection was rotating. After a load of approximately 0.7* $F_{max,est}$, the annular ring shank nails began to pull out noticeably. Tab. 5 shows the increase in deformation on the specimens during the experiment.

Tab. 5: Deformations of timber bracket.

Variant	Specimens	Density ($kg \cdot m^{-3}$)	Deformations I2	
			SCIA w_{100} (mm)	Experiment w_{100} (mm)
V1	1	457	28.05	45.78
	2	362	28.05	39.82
	3	434	28.05	40.83
	4	458	28.05	47.75
V2	1	496	27.06	38.78
	2	555	27.06	30.55
	3	424	27.06	68.92
	4	422	27.06	45.44
V3	1	410	17.11	25.85
	2	466	17.11	28.84
	3	425	17.11	25.62
	4	391	17.11	28.48
V4	1	418	21.36	35.36
	2	418	21.36	42.13
	3	435	21.36	44.65
	4	410	21.36	41.32

Overall, the deformation values are approximately the same in each variant. Slight deviations are due to imperfections in the timber bracket. Wood is an inhomogeneous material and may contain growth knots, resin channels, sudden growth changes and others. These imperfections may locally reduce or increase the strength of the timber, which is reflected in the resulting stiffness and deformation of the timber bracket. The specimens used in the experiment contained a significant amount of growth knots and resin channels.

The deformations in Variant 2 have evolved considerably. The deformations are smallest for specimen 2, which has the highest density. The difference between specimens 1 and 4 is approximately 7 mm, which corresponds to the ratio of the density of the timber brackets. The largest deformations were observed on specimen 3 (Fig. 7), where brittle failure occurred. There was a resin channel in the dowel connection, along which a crack developed.

The calculation of the stiffness of pin and nail connections is based on the stiffness calculation according to the deformation from unit moment method mentioned in (Schickhofer 2006). The connection is loaded with a unit bending moment which causes deformation at the most stressed fastener. Using goniometric functions, the angle of rotation φ of the deformed fastener is calculated from the deformation. By simply calculating the angle of rotation, the stiffness of the connection is calculated.

The value of the bending moment and the value of the deformation of the connection are known from the experiment. The deformation value from sensor I6 is used to calculate the stiffness of the nail connection. The pivot point was estimated at the top edge of the Alumidi connector, which was confirmed in the performed experiments when the top edge of the cantilever was pushed into the glulam beam.

The following table (Tab. 6, Tab. 7) shows the calculated rotational stiffnesses for the dowel and nail parts of the connection from the experiment. The values are compared with the stiffness values from the calculation. The deformation values for calculating the stiffness of the dowel and nail connection were read at the force $F_{max,est}$.

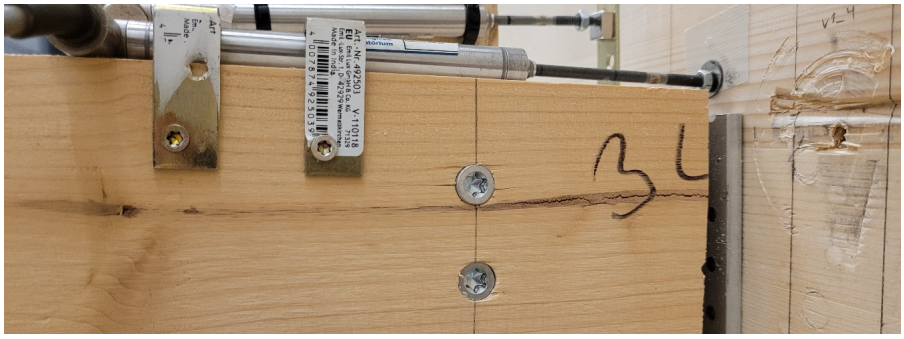

Fig. 7: Brittle failure of specimen 3, variant 2.

Tab. 6: Rotational stiffness from experiment for part A.

Variant	Specimen	Calculation stiffness MSP $C_{\psi,num}$ (MNm·rad^{-1})	Stiffness from experiment MSP $C_{\psi,exp}$ (MNm·rad^{-1})
V1	1	0,0275	0,0128
	2		0,0157
	3		0,0162
	4		0,0134

V2	1	0,0314	0,0175
	2		0,0311
	3		0,0095
	4		0,0161
V3	1	0,0694	0,0287
	2		0,0303
	3		0,0332
	4		0,0301
V4	1	0,0868	0,0441
	2		0,0438
	3		0,0348
	4		0,0352

Tab. 7: Rotational stiffness from experiment for part B.

Variant	Specimen	Calculation stiffness MSP $C_{\psi,num}$ (MNm·rad^{-1})	Stiffness from experiment MSP $C_{\psi,exp}$ (MNm·rad^{-1})
V1	1	0,1351	0,2041
	2		0,2098
	3		0,1579
	4		0,1020
V2	1	0,2201	0,2365
	2		0,2354
	3		0,2076
	4		0,4403
V3	1	0,4643	0,3372
	2		0,3240
	3		0,5778
	4		0,4977
V4	1	0,7780	0,3270
	2		0,2896
	3		0,3561
	4		0,3414

The stiffness from the numerical analysis for the dowel connection was on average 1.69 – 2.26 times greater than the stiffness in the experiment. The stiffness values were balanced across specimens with a scatter of results up to 12%. The exception was Variant 2, where Sample 2 achieved the stiffness value from the numerical analysis and, conversely, Sample 3 had three times less stiffness. For specimen 2, the higher stiffness is due to the high density of up to 555 kg·m^{-3} and the clean cross-section of the timber bracket with no visible knots and resin channels. For specimen 3, the significantly lower stiffness is due to brittle failure of the connection due to a crack in the resin channel in the dowel area.

As for the nail part of the connection, higher stiffness values were observed here from the experiment than from the numerical analysis. The stiffness results are relatively comparable in the different variants. In variant 1, specimen 4 differs, where some nails had to be pre-drilled due to the presence of growth knots in the glulam beam, as the nails could not be applied without breaking through the knots. On the contrary, double stiffness is observed in specimen 4 of variant 2. This is due to improper attachment of the metal plate to the Alumidi bracket. During loading, the plate did not rotate in the same way as the Alumidi bracket.

Interesting results were shown when variant 4 was evaluated. The connection contained the most annular ring shank nails, and the greatest bending stiffness was numerically calculated. The stiffness results from the experiment showed significantly lower values. Upon re-examination of the glulam beam, a crack was found at the bottom of the cross-section which affected the nailing results of Variant 4. The cross section of the beam used will be resawed to determine the crack progression within the cross section.

Subsequently, the calculation of the slip modulus of the connectors was carried out. The results of the dowel section showed values approximately twice lower than those calculated according to the Eurocode 5. After a short reflection, the cause was found, namely in the standard calculation of the slip modulus, where it is possible to multiply the K_{ser} by a factor of 2.0 for steel-timber joints. For self-drilling dowels, which have a special geometry, this factor does not need to be included in the calculation. Consequently, the average stiffness from the experiment is comparable to the results of the numerical analysis. The calculation of the slip modulus of the nail part of the connection showed a larger scatter in the results. Variants 1 and 2 were calculated to have a higher modulus value than the numerical analysis and, conversely, variant 3 had lower modulus values on average. Variant 4 was omitted from the results of the slip modulus due to the mentioned crack in the nail area of the glulam beam.

Tab. 8: Slip modulus for part A.

Variant	Specimen	Slip modulus - calculation K_{ser} ($N \cdot mm^{-1}$)	Slip modulus - experiment K_{ser} ($N \cdot mm^{-1}$)
V1	1	4303.7	2000.2
	2		2461.9
	3		2531.5
	4		2099.3
V2	1	4303.7	2400.8
	2		4261.1
	3		1300.3
	4		2203.5
V3	1	4303.7	1781.5
	2		1877.7
	3		2060.6
	4		1864.9
V4	1	4303.7	2185.5
	2		2174.9
	3		1727.0
	4		1747.8

Tab. 9: Slip modulus for part B.

Variant	Specimen	Slip modulus - calculation K_{ser} ($N \cdot mm^{-1}$)	Slip modulus - experiment K_{ser} ($N \cdot mm^{-1}$)
V1	1	2884.5	4355.9
	2		4478.7
	3		3370.9
	4		2178.1
V2	1	2884.5	3099.6

	2		3085.3
	3		2721.6
	4		5771.6
V3	1	4615.2	3351.9
	2		3220.5
	3		5742.8
	4		4947.1
V4	1	4615.2	1939.8
	2		1717.7
	3		2112.6
	4		2025.3

The average value of the dowel slip modulus from the experiment is 2167.4 $N \cdot mm^{-1}$. If we do not consider the factor of 2.0 for steel- timber joints in the standard calculation, the slip modulus is 2158.8 $N \cdot mm^{-1}$. Therefore, these two values are comparable.

For a more accurate determination of the slip modulus of annular ring shank nails, a larger number of specimens is required.

CONCLUSIONS

In the paper, I discussed semi-rigid connections using the Alumidi connector. Due to its advantages, this new type of connector has considerable application in the load-bearing structures of timber structures. The research was focused on the calculation and experimental verification of the stiffness of the semi-rigid connector, verification of the slip modulus and other factors. Experimentally, 4 variants of the connection have been verified. Each variant contained 4 specimens. In addition to the 16 specimens, 2 preparatory specimens were tested to fine tune the experimental setup and as a presentation for the students.

During the research, the assumption was proven, namely that the Alumidi connectors can be considered as semi-rigid connections.

Throughout the laboratory experiment, the need to carry out a larger number of samples was demonstrated, from the perspective of the next investigation, it would be appropriate to focus on such timber samples that contain defects in order to demonstrate even the most unfavorable situation. The scope of rotational stiffness of samples containing defects could be demonstrated with a larger number of defects samples, it will be necessary due to the declaration of properties of semi-rigid despite connections containing defects.

ACKNOWLEDGMENTS

I would like to thank ROTHO BLAAS SRL, WHC Slovakia s.r.o. and INGSTEEL, spol. s.r.o. for providing the fasteners and material for the experiment.

REFERENCES

1. Dias, A.M., Kuhlmann, U., Kudla, K., Mönch, S., Dias, A.M.A., 2018: Performance of dowel-typ fasteners and notches for hybrid timber structures. Engineering Structures 171: 40-46.
2. Duchoň, V., 2016: Teoretická a experimentálna analýza spojov s vlepovanými tyčami (Theoretical and experimental analysis of joints with glued-in rods). Disertation thesis. Bratislava: SvF STU Bratislava, 80 pp. (In Slovak).
3. Duchoň, V., Klas, T., Katona, O., Brodniansky, J., Balcierák, L., Sandanus, J., Sógel, K., 2016: Experimental tests of timber connections with glued-in rods in bending. Wood Research 61(4): 565-572.
4. Gečys, T., Daniūnas, A., 2017: Rotational stiffness determination of the semi-rigid timber-steel connection. Journal of Civil Engineering and Management 23(8): 1021–1028.
5. Guan, Z.W., Rodd, P.D., 2001: Hollow steel dowels - a new application in semi-rigid timber connections. Engineering Structures 23(1): 110–119.
6. Izzi, M., Flatscher, G., Fragiacomo, M., Schickhofer, G., 2016: Experimental investigations and design provisions of steel-to-timber joints with annular-ringed shank nails for cross-laminated timber structures. Construction and Building Materials 122: 446–457.
7. Izzi, M., Rinaldin, G., Polastri, A., Fragiacomo, M., 2018: A hysteresis model for timber joints with dowel-type fasteners. Engineering Structures 157: 170–178.
8. Jockwer, R., Caprio, D., Jorissen, A., 2022: Evaluation of parameters influencing the load-deformation behaviour of connections with laterally loaded dowel-type fasteners, Wood Material Science & Engineering 17:1, 6-19.
9. Serrano E., Steiger R., Lavisci P., 2008: Glued-in rods. In: Bonding of timber. Core document of the COST Action E34, Wien, 31-39 pp.
10. Larsen, Jensen, J.L., 2000: Influence of semi-rigidity of joints on the behaviour of timber structures. Progress in Structural Engineering and Materials 2: 267-277.
11. Ogrizovic, J., Wanninger, F., Frangi, A., 2017: Experimental and analytical analysis of moment-resisting connections with glued-in rods. Engineering Structures 145: 322–332.
12. Rácz, A., 2017: Experimentálno-teoretické overovanie polotuhých spojov v drevených konštrukciách (Experimental-theoretical verification of semi-rigid joints in timber structures) . Disertation thesis. SvF STU Bratislava, 60 pp. (In Slovak).
13. Sandhaas, C., Munch-Andersen, J., Dietsch, P., Jockwer, R., 2018: Design of connections in timber structures: A state-of-the-art report by COST ActionFP1402 / WG3. European Cooperation in Science and Technology, Aachen, ISBN 978-3-8440-6144-4, 95-318 pp
14. Schickhofer, G., 2006: Holzbau Nachweisführen für Konstruktionen aus Holz. Institut für Holzbau & Holztechnologie Technische Universität Graz.
15. Schweigler, M., Bader, T.K., Hochreiner, G., 2018: Engineering modeling of semi-rigid joints with dowel-type fasteners for nonlinear analysis of timber structures. Engineering Structures 171: 123–139.
16. Solarino, F., Giresini, L., Chang, W.S., Huang, H., 2017: Experimental tests on a dowel-type timber connection and validation of numerical models. Buildings *7*(4): 116.

17. EN 1995-1-1 + A1, 2008: Eurocode 5: Design of timber structures. Part 1-1: General. Common rules and rules for buildings.
18. EN 1993-1-1, 2005: Eurocode 3: Design of steel structures. Part 1-1: General rules and rules for buildings.
19. EN 1993-1-8, 2005: Eurocode 3: Design of steel structures. Part 1-8: Design of joints.
20. EN 383, 2007: Timber structures. Test methods. Determination of embedment strength and foundation values for dowel type fasteners.
21. EN 380, 1998: Timber structures. Test methods. General principles for static load testing.
22. Tlustochowicz, G., Serrano, E., Steiger, R., 2011: State-of-the-art review on timber connections with glued-in steel rods. Materials and Structures/Materiaux et Constructions 44(5): 997–1020.
23. Xu, B.H., Bouchaïr, A., Racher, P., 2012: Analytical study and finite element modelling of timber connections with glued-in rods in bending. Construction and Building Materials 34: 337–345.
24. Zöllig, S., Frangi, A., Franke, S., Muster, M., 2016: Timber structures 3.0. New technology for multi-axial, slim, high performance timber structures. WCTE 2016 - World Conference on Timber Engineering, (22-25 August, Vienna), 9 pp.
25. Jockwer R., Serrano E., 2021: Glued-in rods as reinforcement for timber structural elements. Reinforcement of Timber Elements in Existing Structures, 29-49 pp

MATÚŠ NEUSCH, JAROSLAV SANDANUS*, KLARA FREUDENBERGER
SLOVAK UNIVERSITY OF TECHNOLOGY IN BRATISLAVA
FACULTY OF CIVIL ENGINEERING
DEPARTMENT OF STEEL AND TIMBER STRUCTURES
RADLINSKÉHO 2766/11
810 05 BRATISLAVA
*Corresponding author: jaroslav.sandanus@stuba.sk